











# GAMBUT field experiment of peatland wildfires in Sumatra: from ignition to spread and suppression

Muhammad A. Santoso<sup>A,E</sup> , Eirik G. Christensen<sup>A</sup> , Hafiz M. F. Amin<sup>A,B</sup> , Pither Palamba<sup>C</sup> , Yuqi Hu<sup>A,D</sup>,  
Dwi M. J. Purnomo<sup>A</sup> , Wuquan Cui<sup>A</sup> , Agus Pamitran<sup>E</sup>, Franz Richter<sup>A</sup> , Thomas E. L. Smith<sup>F</sup> ,  
Yulianto S. Nugroho<sup>E</sup>  and Guillermo Rein<sup>A,\*</sup> 

For full list of author affiliations and declarations see end of paper

**\*Correspondence to:**

Guillermo Rein  
Department of Mechanical Engineering,  
and Leverhulme Centre for Wildfires,  
Environment and Society, Imperial College  
London, London, SW7 2AZ, UK  
Email: [g.rein@imperial.ac.uk](mailto:g.rein@imperial.ac.uk)

## ABSTRACT

Peat wildfires can burn over large areas of peatland, releasing ancient carbon and toxic gases into the atmosphere over prolonged periods. These emissions cause haze episodes of pollution and accelerate climate change. Peat wildfires are characterised by smouldering – the flameless, most persistent type of combustion. Mitigation strategies are needed in arctic, boreal, and tropical areas but are hindered by incomplete scientific understanding of smouldering. Here, we present GAMBUT, the largest and longest to-date field experiment of peat wildfires, conducted in a degraded peatland of Sumatra. Temperature, emission and spread of peat fire were continuously measured over 4–10 days and nights, and three major rainfalls. Measurements of temperature in the soil provide field experimental evidence of lethal fire severity to the biological system of the peat up to 30 cm depth. We report that the temperature of the deep smouldering is ~13% hotter than shallow layer during daytime. During night-time, both deep and shallow smouldering had the same level of temperature. The experiment was terminated by suppression with water. Comparison of rainfall with suppression confirms the existence of a critical water column height below which extinction is not possible. GAMBUT provides a unique understanding of peat wildfires at field conditions that can contribute to mitigation strategies.

**Keywords:** fire behaviour, emission, spread, haze, peat, slash-and-burn, smouldering, suppression.

## Introduction

Peat is organic soil formed by long term natural accumulation of decayed vegetation, and peatlands are the largest reserves of terrestrial organic carbon (Turetsky *et al.* 2015; Rieley and Page 2016). Peatlands occupy up to 3% of the Earth's land surface but store around 25% of the world's soil carbon (Yu 2012). Peat formation occurs in ecosystems that are either often flooded by water, as in the case of tropical peatlands, or in cold climate conditions as in boreal and Arctic peatlands (Page *et al.* 2011; Yu 2012; Turetsky *et al.* 2015). However, peat can be flammable when dry or thawed and wildfires can be ignited by natural events such as lightning (Mickler *et al.* 2017) and self-heating (Restuccia *et al.* 2017), or anthropogenic activities such as land clearing, accidental burning, and arson (Page *et al.* 2002, 2011; Rein 2016). Their spread is governed by smouldering combustion, and fires can last for weeks or months despite rainfall or firefighting (Page *et al.* 2002; Huijnen *et al.* 2016; Rein and Huang 2021) (see Fig. 1). Smouldering is the slow, low temperature, flameless burning of porous fuels (Ohlemiller 1985; Rein 2016). During the 1997 haze episode in Southeast Asia, peat fires released up to ~2570 Tg of carbon, which is equivalent to 40% of annual global emissions (Page *et al.* 2002). The recent 2015 haze episode in Southeast Asia released  $227 \pm 67$  Tg of Carbon, with an average rate of daily CO<sub>2</sub> emission exceeding the fossil fuel emission rate of the European Union (Huijnen *et al.* 2016). Annually, drained peatlands release ~5% of global anthropogenic greenhouse gas emissions (IUCN 2017), which, considering the very long period of 100–1000 years needed for the carbon in peatland to be stored,

**Received:** 6 October 2021

**Accepted:** 7 August 2022

**Published:** 28 September 2022

**Cite this:**

Santoso MA *et al.* (2022)  
*International Journal of Wildland Fire*  
31(10), 949–966. doi:10.1071/WF21135

© 2022 The Author(s) (or their employer(s)). Published by CSIRO Publishing on behalf of IAWF. This is an open access article distributed under the Creative Commons Attribution 4.0 International License (CC BY)

OPEN ACCESS

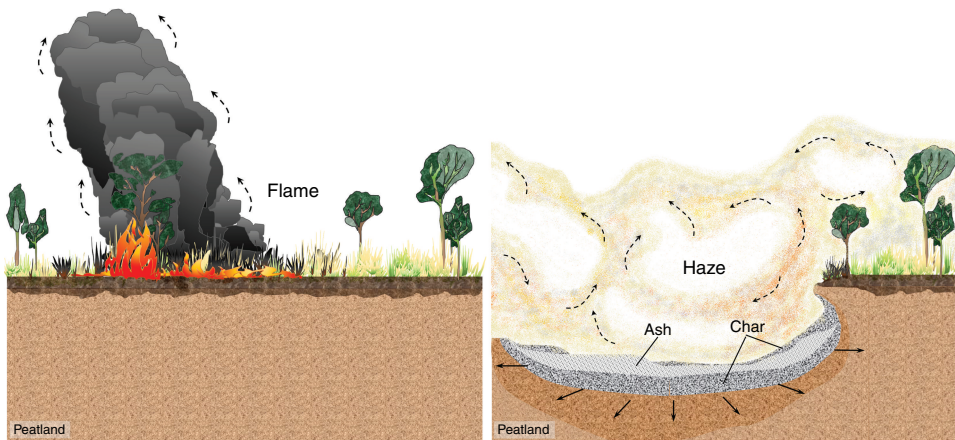


**Fig. 1.** Flaming (left) and smouldering (right) wildfires in a peatland. Peat wild-fire ignition can be caused by anthropogenic activities such as land clearing, accidental burning, arson, or natural causes like lightning strike or self-heating. The illustration is taken from Hu *et al.* (2018) (image by Y. Hu).

contribute to the acceleration of climate change (Kelly *et al.* 2013; Rein 2013; Gandois *et al.* 2019; Walker *et al.* 2020; Rein and Huang 2021).

Various scales of experiments are required to understand peat fires (Christensen *et al.* 2019), so that effective and efficient mitigation efforts can be formulated. At the micro-scale, in the order of milligram samples, the fundamental chemistry of smouldering peat has been identified, revealing exothermic and endothermic reactions (Chen *et al.* 2011; Huang and Rein 2014). At the mesoscale, in the order of gram to kilogram samples, the studies are on the dynamics of peat fire such as the critical ignition limits based on moisture content (MC) and inorganic content (IC) (Frandsen 1987, 1997; Rein *et al.* 2008), horizontal and in-depth spread (Huang *et al.* 2016; Prat-Guitart *et al.* 2016a, 2016b; Christensen *et al.* 2020), gaseous emission (Hu *et al.* 2019), and suppression (Ramadhan *et al.* 2017; Lin *et al.* 2020; Santoso *et al.* 2021). Currently, the maximum characteristic length of laboratory mesoscale studies in the literature is 40 cm (Benscoter *et al.* 2011; Huang and Rein 2019; Christensen *et al.* 2020). Although these investigations in the micro and mesoscale provide fundamental understanding of peat fire behaviours, they were conducted in artificial laboratory conditions as compared with the natural conditions where variables change significantly over time and space. Thus, experimental evidence at the field scale is essential to bridge between understanding in the mesoscale to the real landscape.

Field-scale studies of peat fires have been previously conducted post-fire (Page *et al.* 2002; Usup *et al.* 2004; See *et al.* 2007; Huijnen *et al.* 2016; Simpson *et al.* 2016; Smith *et al.* 2018), with minimum *in situ* measurements. The origin and end of the fires (essential elements of fire dynamics analysis) in these studies were generally unknown. Pastor *et al.* (2017) conducted systematic experiments in peatland in the Peruvian Andes, in plots of 50 × 50 cm. Even though the experimental location is in the field, this sample size is as small as laboratory scale. Only three out of 18 tests registered temperatures above 100°C, and only one

recorded temperature up to 400°C, indicating that only one fire spread but all others did not ignite. Thus, taking all these studies together, the information required to understand the actual behaviour of real peat fire, its spread despite rainfalls and firefighting response, is still minimal.

Here, we report GAMBUT (Indonesian word for ‘peat’), the experiments of tropical peat fires in the field and the largest-to-date peat fire experiments. Gambut considered and measured field-scale peat fire behaviour in terms of temperature, fire area, spread rate, emissions, and suppression. The location is a secondary peat swamp forest in Sumatra Island of Indonesia. Indonesia contains the largest share of peat carbon in Southeast Asia (65%, 57.4 Gt) in which peatland fires have frequently spread (Gaveau *et al.* 2014; Tacconi 2016; Iriana *et al.* 2018; Hoyt *et al.* 2020). Secondary or degraded peatland is the result of disturbed pristine peatland due to logging, deforestation, and draining (Murdiyarto *et al.* 2019). The total experimental area was 408 m<sup>2</sup>. The shortest and longest fires observed in this study were 4 and 10 days, respectively, up until controlled suppression. GAMBUT is the first study to fill the gap in the understanding of peat fire dynamics between laboratory and field scale, and provide field evidence to formulate an effective and efficient mitigation response.

## Material and methods

### Field site and experimental plots

The field experiment was conducted in Rokan Hilir regency, Sumatra, Indonesia, from 19 to 29 August 2018. The location of the site experiment was determined according to field surveys and correspondence with the Ministry of Interior of the Republic of Indonesia. The dates of the experiment were chosen for favourable conditions for peat fire, as suggested by climate data, with an average temperature of 27.4°C (minimum 23.4°C, maximum 33°C) and an average relative humidity of 79.1 ± 4.9% in the previous 5 years (BMKG 2022). The dates of the experiment also made

possible the investigation of the effect of rainfall because the rainy season tends to start at the end of August (Badan Pusat Statistik Kabupaten Rokan Hilir 2015; BMKG 2022).

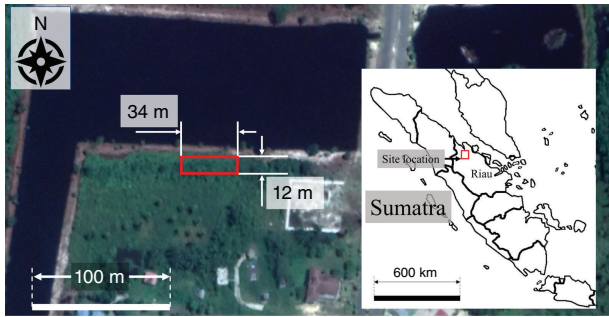


**Fig. 2.** Top view of the site for GAMBUT experiment near a reservoir (Source: Balai Diklat Satpol PP dan Damkar, Rokan Hilir, Riau, Kementerian Dalam Negeri Republik Indonesia. (1°36'17.1"N 100°58'30.5"E). Google Earth, 18 October 2017. 26 May 2022.). The experiment area is indicated by the red rectangle. The site is a secondary peat swamp forest in Rokan Hilir, Sumatra, Indonesia (1°36'17.1"N 100°58'30.5"E). Inset picture shows Sumatra Island in which the site is indicated by a red rectangle.

The site in this study is in a tropical wet climate with a mean annual rainfall of 2080 mm (Badan Pusat Statistik Kabupaten Rokan Hilir 2015); it is mostly covered by palm trees, ferns, and sedges, and is in the vicinity of a water reservoir (pond) (Fig. 2). From the weather data of the previous 5 years, drought season occurs in June and July with monthly rainfall at ~85 mm, which starts to increase in August (Badan Pusat Statistik Kabupaten Rokan Hilir 2015). The mean daily rainfall in August is 6.5 mm with the maximum daily rainfall of 117.2 mm (BMKG 2022).

Fig. 3a shows the chronology of this experiment, which was conducted over 12 days and nights across changing precipitations (Fig. 3b) and weather patterns (Fig. 3c). Measurements from the installed weather station on site show that the average intensity of rainfall occurred in the afternoon of Day 6 (17:20 hours Western Indonesian Time (WIT)), the night of Day 6 (21:36 hours WIT), and the night of Day 9 (21:26 hours WIT), and were 5.6, 1.4, and 8.3 mm/h respectively (Fig. 3b). These three rainfall events equated to 4.8 mm of water column height in the afternoon of Day 6, 1.4 mm in the night of Day 6, and 2.5 mm in the night of Day 9. The maximum ambient temperature was

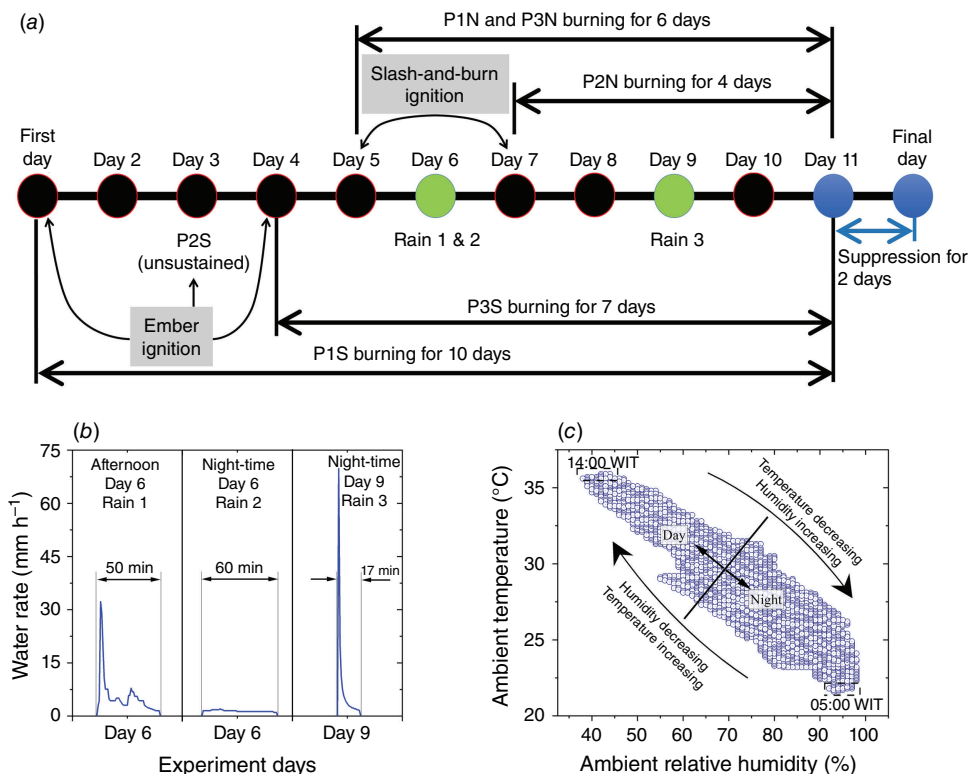


**Fig. 3.** (a) Chronology of GAMBUT experiments from ignition to suppression. The field experiment was conducted over 12 days: the first 10 days for free burning and the last 2 days for suppression. Plot 1 North (PIN), Plot 2 North (P2N), Plot 3 North (P3N), Plot 1 South (PIS), Plot 2 South (P2S), and Plot 3 South (P3S) are the fire areas in Fig. 4a and Table 2. (b) Evolution of water rate for three recorded rainfall events on Day 6 and 9. (c) Recorded ambient temperature and relative humidity from Day 1 to 12. WIT is Western Indonesia Time (GMT + 7 h). Daytime period is determined from 05:00 to 18:00 hours WIT and night-time is from 18:00 to 05:00 hours WIT.



35.9°C and the minimum was 21.6°C (Fig. 3c). The maximum air relative humidity was 98% with a minimum of 38%. Considering that the difference between the maximum and minimum temperature, and of air relative humidity, was 14.3°C and 60%, these experiments include data over significant changes of environmental conditions, including dry-hot and humid-cold moments of the day.

In total, six peat fire experiments were conducted. The experiments were conducted in three plots of land, each with dimensions of 10 × 10 m (Fig. 4a). From the left to right of Fig. 4a, the plots are indicated as Plot 1, Plot 2, and Plot 3. In each plot, two peat fire experiments were conducted (Fig. 4b): Plot 1 North (P1N) and Plot 1 South (P1S); Plot 2 North (P2N) and Plot 2 South (P2S); and Plot 3 North (P3N) and Plot 3 South (P3S). The topography of the plots shows an elevation difference of ~1 m between the south and north sides (Fig. A2 in the Supplementary Appendix). Firebreaks were made around the perimeter of each plot by digging trenches of 50 cm wide and 50 cm deep, filled with sand to prevent fires from spreading beyond each plot. Fires in the north and south sides of the plots were separated and did not spread into each other.

Plot surfaces were cleaned from palm trees, ferns, sedges, and surface litter vegetation, except Plot 1, where surface

litter vegetation (duff) was kept intact (Fig. 4b) to observe its effect on slash-and-burn. Fig. 4a shows that the litter vegetation left on Plot 1 had dried naturally and turned brownish, similar to the colour of dried peat in Plot 2 and Plot 3. Visual observation of the different surface treatment between Plot 1 and other plots from up-close can be seen in Fig. A1 in the Supplementary Appendix.

### Peat properties investigations

Pre-experiment peat sampling was conducted to measure bulk density, moisture content (MC), elemental content (C/H/N), and inorganic content (IC). Sampling locations are shown in Fig. 4a and were chosen to investigate properties' variations caused by topography differences between the north and south sides of the plots (Fig. A2 in the Supplementary Appendix). Samples were taken at four depths: 0–10, 10–20, 20–30, and 30–40 cm, using a cylindrical corer of 2.54 cm diameter and 10 cm length. These depths were chosen based on the range of depth of burn of peat fire recorded in the literature from 1983 to 2015 (Santoso et al. 2019). The samples were immediately weighed to measure the wet bulk density ( $\rho_{wet}$ ). Volumetric moisture content (VMC) was measured by Delta-T SM150T soil moisture sensor probe (Delta-T Devices Ltd, England), with an accuracy of ± 3%. Using the measured bulk density, the moisture content (MC) in dry-mass basis was calculated using Eqn 1 where  $\rho_{H_2O}$  is water density of 1000 kg m<sup>-3</sup>.

$$MC = \frac{1}{\frac{\rho_{wet}}{VMC \times \rho_{H_2O}} - 1} \quad (1)$$

After the bulk density was measured, a subsample of ~10 g was taken to measure the C/H/N content using CE440 Elemental Analyzer (Exeter Analytical (UK) Ltd, England). The rest of the sample was then used for the measurement of IC, using the Loss on Ignition (LoI) method by burning the sample in a furnace at 1000°C (Christensen et al. 2020). Before the LoI, the sample was dried in an 80°C oven for 48 h so that the IC measurement was conducted in dry-mass basis. The dry sample was then heated in the furnace until no mass loss was detected. Table 1 shows the summary of the peat properties investigations.

### Spread measurements

Thermocouples were used to measure smouldering temperature, and to investigate thermal residence time and spread rate. Due to the uncertainty of the direction of peat fire spread, thermocouples were placed based on the visual observation of the fire and the likely direction of spread. To obtain spread rate data, thermocouple points were located 15 cm apart. The spread rate was then calculated from the known distance, and the time-lapse of when two consecutive thermocouples reached their maximum

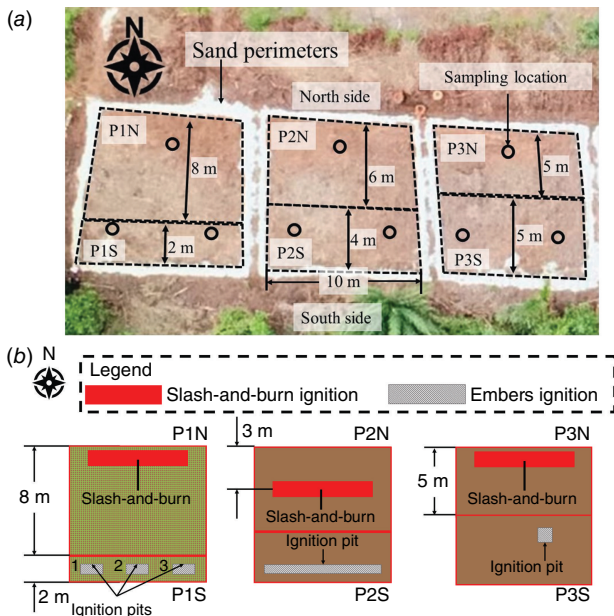


**Fig. 4.** (a) Top view of the 12 × 34 m of experimental area after surface vegetation treatment. Black circles represent peat sampling locations for measurements of bulk density, moisture content (MC), inorganic content (IC), and elemental content. (b) Schematic of the fire areas and different ignition methods. Red and grey rectangles refer to slash-and-burn and embers ignitions, respectively. Square grids in PIN refer to the surface litter that is kept intact on Plot 1. Fire areas indicated by P1N, P2N, P3N, P1S, P2S, and P3S are Plot 1 North, Plot 2 North, Plot 3 North, Plot 1 South, Plot 2 South, and Plot 3 South, respectively.



**Table 1.** Physical and chemical properties of peat in this study.

Measurement locations	Measurement depth (cm)	$\rho_{b,wet}$ (kg m <sup>-3</sup> )	Moisture content (% dry mass basis)	Elemental analysis			Inorganic content (%)
				C (%)	H (%)	N (%)	
PIN	0–10	1136	150.9	33.73	3.2	0.88	44.8
	10–20	1230	191.2	30.73	16.46	0.82	23.6
	20–30	1458	153.3	25.97	10.21	0.62	NM
	30–40	1483	200.3	NM	NM	NM	NM
PIS	0–10	656	32.3	21.94	2.43	0.57	63.5
	10–20	766	39.0	23.81	2.48	0.55	57.6
	20–30	793	64.6	26.05	2.11	2.51	54.9
	30–40	879	78.2	NM	NM	NM	NM
P2N	0–10	921	77.5	22.56	3.86	0.69	49.5
	10–20	934	231.8	34.77	6.34	1.69	NM
	20–30	1243	292.1	36.56	6.67	1.53	38.4
	30–40	1389	458.0	NM	NM	NM	NM
P2S	0–10	714	24.1	22.37	2.66	0.63	53.2
	10–20	776	41.0	17.89	3.46	0.5	NM
	20–30	890	55.6	24.76	5.39	0.74	53.5
	30–40	1037	54.7	NM	NM	NM	NM
P3N	0–10	737	91.9	23.22	2.66	1.09	49.8
	10–20	905	189.8	32.92	3.38	1.57	NM
	20–30	1455	126.1	22.21	8.34	0.61	55.0
	30–40	1478	197.0	NM	NM	NM	NM
P3S	0–10	806	18.9	17.19	1.81	0.49	71.2
	10–20	925	27.3	14.2	1.53	0.4	NM
	20–30	991	35.3	17.98	1.96	0.46	62.3
	30–40	988	50.9	NM	NM	NM	NM

The sampling locations are shown in Fig. 4a. NM, not measured.

temperature (Torero and Fernandez-Pello 1996) or reached 300°C, which is above peat char oxidation temperature (230°C; Chen *et al.* 2011). Each thermocouple point contained two K-type thermocouples at 10 cm (shallow layer) with probe diameter of 1.5 mm, and at 30 cm depth (deep layer) with probe diameter of 3 mm. Details of thermocouple placement can be seen in Fig. A3 in the Supplementary Appendix. As the fire progressed past a thermocouple point, it was then moved to a new location.

Thermal residence time is the duration of time for which a recorded temperature at a measurement point is greater than a specified temperature threshold (Rein *et al.* 2008). In this study, the threshold was varied from 200°C up to 700°C. The 200°C temperature threshold is above the onset of peat pyrolysis temperature, but below peat char oxidation (Chen *et al.* 2011).

Infrared (IR) images were recorded using a FLIR Duo-R camera (FLIR Systems UK, England), mounted on a crane

with adjustable field of view. The crane was mounted on rails to allow for imaging the whole site (Fig. 5). The field image acquisition can be seen in Fig. A5 in the Supplementary Appendix. Fire locations on the surface were measured by analysing the IR images using a similar approach to that in Amin *et al.* (2020). The images were converted to greyscale and the pixels were marked where the normalised intensity increased above an intensity threshold (subset in Fig. 5). The area of all the marked perimeter was then determined to be the fire area. The scaling from pixel dimension to physical length was made possible by using a geo-reference with a dimension of 0.17 × 0.14 m, also shown in the subset of Fig. 5.

Depth of burn (DOB) measurement is shown in Fig. A4 in the Supplementary Appendix, and was conducted by burying a thin metal pole with a geo-reference plate attached on the top, flush with the top of the peat layer. The poles were located every 2 m. The measurements of DOB were taken on day 12, after the field experiment was terminated, by

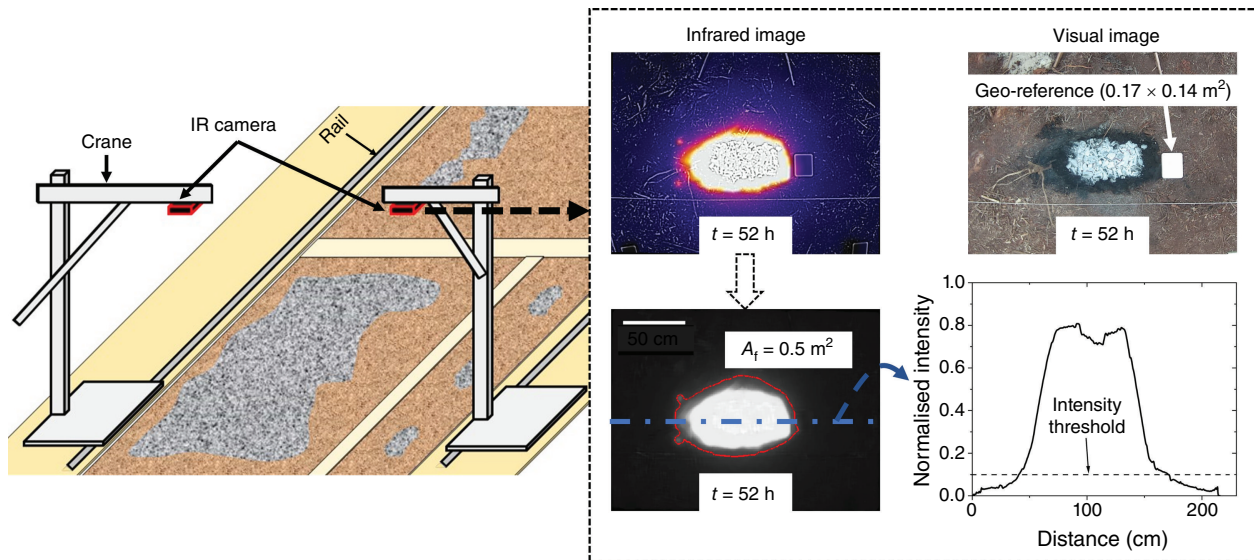


**Fig. 5.** Infrared imaging setup and analysis to measure smouldering spread and area. The normalised pixel intensity threshold is chosen to be 0.1 to represent the point at which the intensity started to steeply increase, indicating the outer perimeter of the peat fire area.  $A_f$  and  $t$  are fire area and time since ignition respectively.

measuring the distance between the plate and the layer of the peat.

The gaseous emissions were measured by using open-path Fourier transform infrared spectroscopy (OP-FTIR), consisting of a M2000 Series equipped with a Stirling-cooled mercury–cadmium–telluride detector and fitted with a MIDAC custom-built 76 mm Newtonian telescope (MIDAC Corporation, Westfield, MA, USA). The spectrometer was mounted onto an adjustable tripod to provide stable support facilitating the signal reception from a remotely located infrared source, consisting of a 12 V silicon carbide glow bar operating at 1500 K fitted in front of a 20 cm diameter gold-plated collimator (Smith *et al.* 2018). Each data output from the OP-FTIR is the result of 16 scans at every  $\sim 18$  s. The quantification of emission factors (EFs) (grams of emitted species per kilogram of dry fuel) of  $\text{CO}_2$ ,  $\text{CO}$ ,  $\text{CH}_4$ ,  $\text{NH}_3$ , and  $\text{HCN}$  are based on the carbon balance approach detailed in Paton-Walsh *et al.* (2014) and Smith *et al.* (2014, 2018). Each measurement of the emission factor was conducted over 10–110 min (details of locations and number of measurements can be seen in Table A1, Supplementary Appendix).

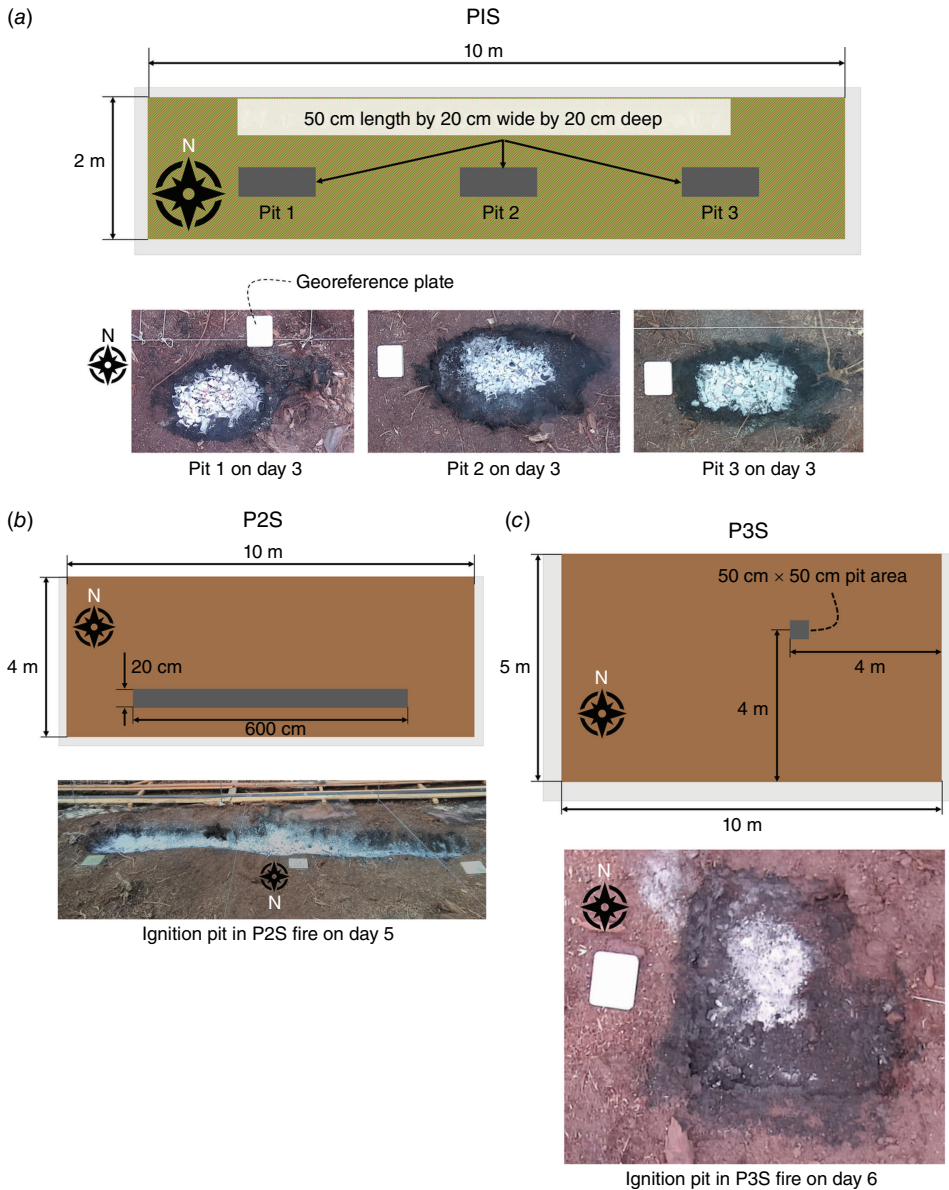
### Fire area and ignition methods

Ignitions were attempted either by deposition of charcoal embers or slash-and-burn. In the case of charcoal embers, the particles of charcoal were ignited with gasoline and left to burn for 10 min, and then put into the ignition pit. This ignition method was conducted in P1S, P2S, and P3S. There were three pits in P1S, each with dimensions of  $0.5 \text{ m} \times 0.2 \text{ m}$  and  $0.2 \text{ m}$  deep (Fig. 6a), the pit in P2S was  $6 \text{ m} \times 0.2 \text{ m}$  and  $0.2 \text{ m}$  deep (Fig. 6b), and the one in P3S

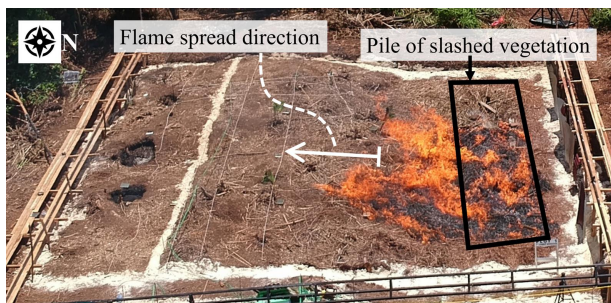
was  $0.5 \text{ m} \times 0.5 \text{ m}$  and  $0.4 \text{ m}$  deep (Fig. 6c). A total of 9.3 kg of charcoal was used to produce the embers that were put in each of the pits in P1S, 70 kg in P2S, and 16 kg in P3S. In P3S, the ember ignition was aided by additionally burning 500 mL of gasoline (once the embers were already in the pit), resulting in flames of 1.5 m height for  $\sim 15$  min.

Fig. 6a, c shows ember-ignited peat fire in P1S and P3S 2 days after ignition. On Day 3, the fire of the three pits in P1S had grown significantly from  $0.1 \text{ m}^2$  before ignition to  $0.42$ ,  $0.6$ , and  $0.5 \text{ m}^2$  for Pit 1, 2, and 3 respectively. In P3S, the fire size increased from  $0.25$  to  $0.46 \text{ m}^2$  in 2 days. These increases in fire size indicate self-sustaining smouldering. The ignition attempt in P2S did not result in a sustained fire, as shown by the absence of size increase (Fig. 6b). During digging on Day 12, no hotspots were found in the layer of ash or below. The longest self-sustained peat fire in this study was the ember-ignited fires on the south side of plot 1 (P1S, Fig. 4b), which lasted for 10 days.

Slash-and-burn ignition was attempted in P1N, P2N, and P3N by burning dried tree branches, sedges, and litters put together in a pile with dimensions of 8 m in length, 1 m wide, and 0.5 m high (Fig. 7). This ignition mode was chosen because most occurrences of smouldering fires in peatland start with the burning of agricultural waste (Page *et al.* 2011). During the conversion of peatland into a plantation site, the native surface vegetation is slashed and burned, hence the name slash-and-burn, which is the cheapest way to convert the land. Every few years, this land conversion activity results in regional-scale pollution called haze, driven by smouldering peat fires and made worse by a longer and warmer drought season due to El Niño (Page *et al.* 2002; Huijnen *et al.* 2016; Hu *et al.* 2018).



**Fig. 6.** Attempts at ember ignition in (a) PIS area with bottom figure showing peat fires on day 3, (b) P2S area with bottom figure showing un-sustained peat fire on day 5, and (c) P3S area with bottom figure showing peat fire on day 6. Grey rectangle is the ignition location.



**Fig. 7.** Slash-and-burn ignition on PIN on day 5. The surface vegetation of PIN was not removed, which resulted in flame spread beyond the biomass pile and also ignited the peat. The sand perimeter was to stop flames from PIN into PIS.

Slash-and-burn was conducted on the north side of the plots (Fig. 4b) to observe the induced smouldering peat fire employing a strong ignition source because the MC and bulk density of the north side of the plot were found to be significantly higher than the south side (Table 1). A sand line perimeter was introduced between P1N and P1S (Fig. 7) to stop the flames spreading from slash-and-burn ignition in P1N to P1S. Such a line was not introduced in Plot 2 and Plot 3 because the slash-and-burn in P2N and P3N were not as intense as in P1N. All slash-and-burn ignition attempts resulted in self-sustained peat fire (Fig. 3a).

In addition to MC measurement before ignition, continuous MC measurements were made in P2N area by placing soil moisture sensors at four different depths (10, 20, 30, and 40 cm) below the slash-and-burn location (Fig. 4b).



**Table 2.** Summary of fire area dimensions, ignition methods, and period of each fire experiment.

Fire area	Dimension		Type	Size	Ignition method	Period	
	Start	End				Start	End
Plot 1 North (P1N)	10 m × 8 m	10 m × 8 m	Slash-and-burn	8 m × 1 m by 50 cm high		Day 5	Day 11
Plot 2 North (P2N)	10 m × 6 m	10 m × 6 m				Day 7	Day 11
Plot 3 North (P3N)	10 m × 5 m	10 m × 5 m				Day 5	Day 11
Plot 1 South (P1S)	10 m × 2 m	10 m × 2 m	Ember ignition	Three ignition pits. Each pit had dimension of 0.5 m × 0.2 m and 0.2 m deep, and each was filled with embers from ~9.3 kg of activated charcoal		Day 1	Day 11
Plot 2 South (P2S)	10 m × 4 m	10 m × 4 m	Ember ignition	One ignition pit with dimension of 6 m × 0.2 m and 0.2 m deep. The pit was filled with embers from 70 kg of activated charcoal		Day 3	Unsustained smouldering
Plot 3 South (P3S)	10 m × 5 m	10 m × 5 m	Ember ignition	One ignition pit with dimension of 0.5 m × 0.5 m and 0.4 m deep. The pit was filled with embers from 16 kg of activated charcoal. Ignition was also aided by burning 500 mL of gasoline		Day 4	Day 11

Illustration of the fire area can be seen in Fig. 4.

Measurement of MC ahead of a smouldering fire in real-time has not been done before in the literature. Table 2 shows the summary of the dimensions of the area, the ignition methods, and the start and end of each experiment.

## Suppression

Controlled suppression was applied on Day 11 (Fig. 3a) with water spray and lance injection methods. The suppression was applied using a fire hose and a fire pump. The average flow rate was calibrated by filling a container with known volume and noting the duration needed for filling it up at a specified pump discharge pressure. Water spray suppression was applied on P1N, P2N, P3N, and P3S. The flow rate for water spray on P1N, P2N, and P3N was  $3024 \pm 18 \text{ L h}^{-1}$  and on P3S was  $4878 \pm 120 \text{ L h}^{-1}$ . Suppression was applied for 1 h in P1N, P2N, and P3N.

Lance injection was applied to the three pits of P1S (Fig. 4b) by connecting the fire hose to a lance injection device. The flow rate during lance injection suppression was  $1669 \text{ L h}^{-1}$  and applied for 25 min in Pit 1 of P1S, 35 min in Pit 2 of P1S, and 13 min in Pit 3 of P1S.

During suppression, a portable thermocouple was used to survey in-depth temperatures in the area. The exact suppression duration was then estimated by time since water delivery was started to the time when temperature recorded by in-depth thermocouple (located as in Fig. 8 for P1N, P2N, and P3N; and as in Fig A6 in the Supplementary Appendix for P1S and P3S) decreased below  $50^\circ\text{C}$ , which was chosen as a conservative extinction threshold previously used to avoid reignition (Santoso et al. 2021). After the suppression, all the surveyed points recorded temperatures below  $50^\circ\text{C}$ .

## Results and discussion

### Surface treatment and smouldering spread

P1N experimental plot containing a duff layer of litter vegetation resulted in the largest and longest flaming spread compared with plots that were cleared of vegetation (P2N and P3N, Fig. 8). The flames spread farther than the initial piles of slashed vegetation, causing the peat fire to be larger than the initial pile (Figs 7, 8a). When the litter was removed as in P2N and P3N, peat burned only around the location of the initial pile, even after 6 days of slow spread (Fig. 8b, c). This confirms transition from flaming to smouldering, which is the process in which the flaming duff layer causes the smouldering hotspot in peat layer below (Purnomo et al. 2021).

The peat fires in this study sustained from a few hours up to 40 h at any single location (Fig. 9). Measurements of the thermal residence time showed that in plots where litter was cleared, peat fire in the shallow layer (10 cm deep) was weaker than in the deep layer (30 cm deep) (P3N in Fig. 9b). However, the residence time in the deep layer

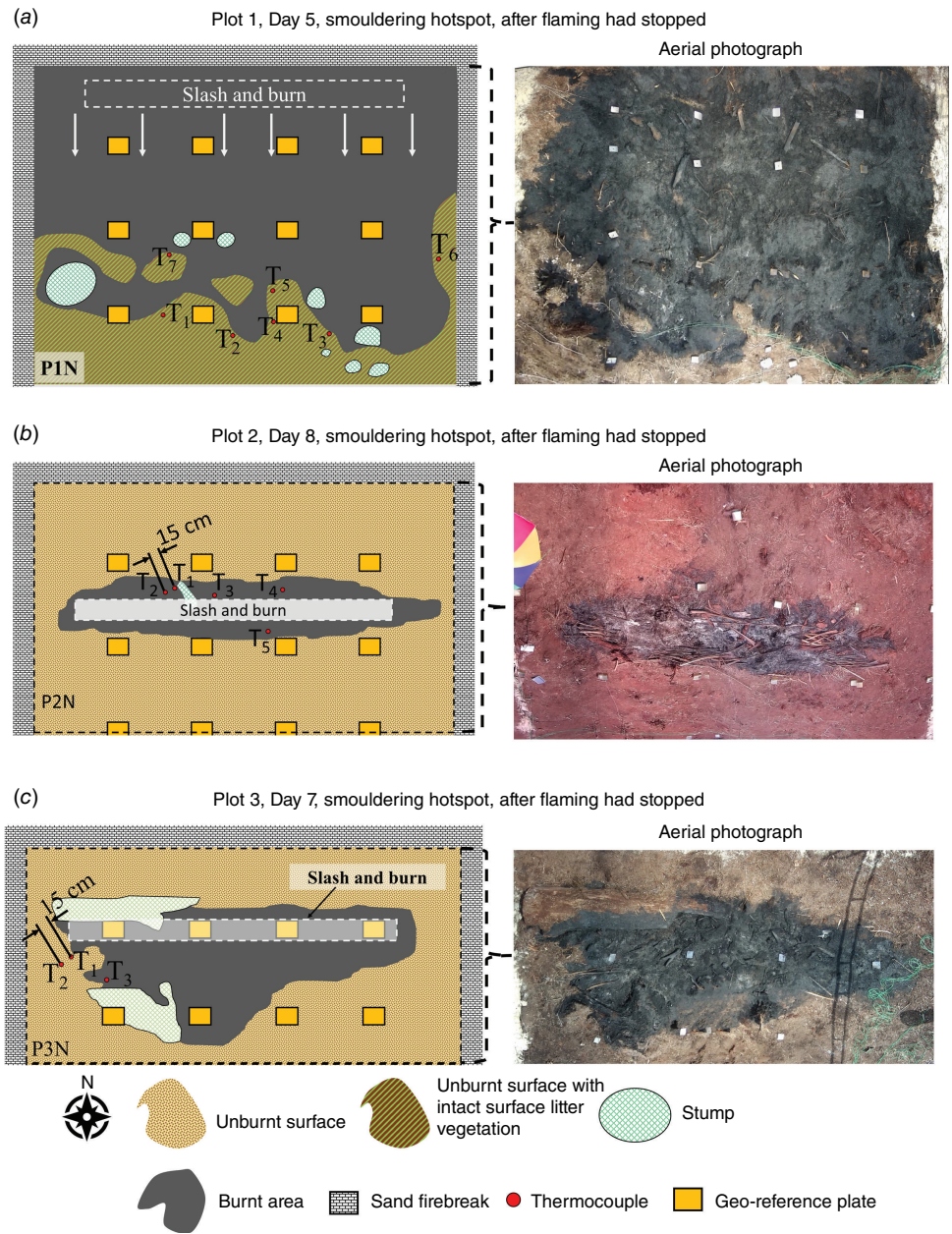


**Fig. 8.** Sketch of thermocouples locations (red dots) and fire (grey shade) after slash-and-burn ignition. The pictures on the right-hand side are aerial photographs. (a) PIN on Day 5 showing peat fire due to slash-and-burn ignition. The aerial photograph of PIN was taken on Day 7. The thermocouple locations in PIS fire can be seen in Fig. A6a in the Supplementary Appendix. (b) P2N on Day 8 showing peat fire due to slash-and-burn ignition. The aerial photograph of P2N was taken on Day 8. Thermocouples were not put in P2S because the fire was not self-sustained. (c) P3N on Day 7 showing peat fire due to slash-and-burn ignition. The aerial photograph of P3N was taken on Day 7. The thermocouple locations in P3S fire can be seen in Fig. A6b in the Supplementary Appendix. Yellow rectangles are geo-reference plates (size  $0.17 \times 0.14 \text{ m}^2$ ). Dashed white rectangle is the location of slash-and-burn ignition.

(30 cm in Fig. 9b) of cleared plots (represented by P3N) was similar to that of P1N (30 cm deep in Fig. 9a). This indicates that despite the less intense burning of the surface, peat fire in the deep layers can have a high severity if self-sustained.

This self-sustained peat fire occurred even though the initial MC ranged from 100 to 200% in dry-mass base (Table 1), reaching peak temperature around  $700^\circ\text{C}$  (Fig. A8 in Supplementary Appendix).

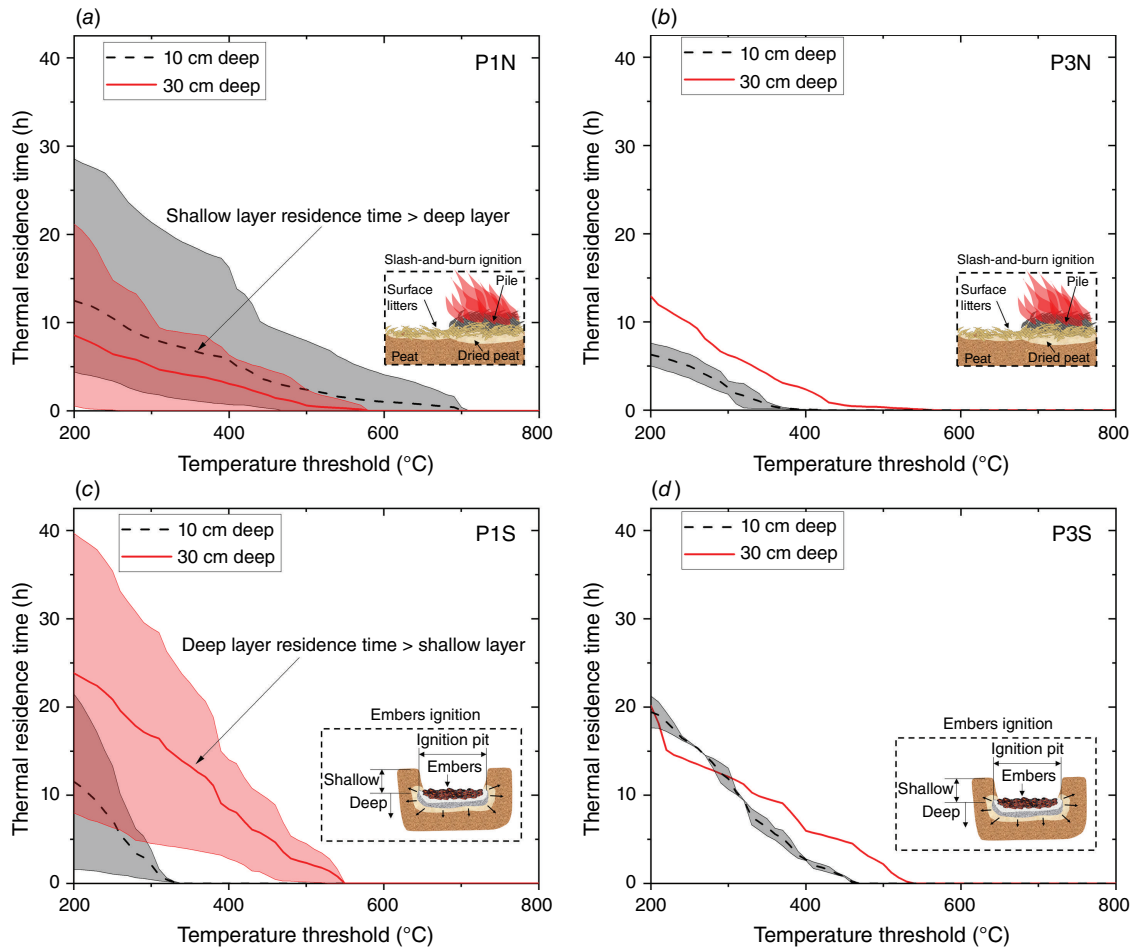


**Fig. 9.** Fire severity in the peat measured as the thermal residence time due to smouldering after slash-and-burn ignition in (a) P1N and (b) P3N. Thermal residence time due to smouldering after ember ignition in (c) P1S and (d) P3S. Shading spans the minimum and maximum range of values.

Examining the thermal residence time for the 300°C threshold results in an average of 12–17 h of deep smouldering initiated by ember ignition (Fig. 9c, d), and an average of 2.5–8 h with a maximum of ~21 h of shallow smouldering initiated by slash-and-burn (Fig. 9a, b). These results indicate the severe effects of the fires and the potentially important disturbance agent in the ecosystems (Rein et al. 2008; Muñoz-Rojas and Bárcenas-Moreno 2019; Santoso et al. 2019). It has been reported before that thermal residence time of 2 h at 160°C or more is lethal to the soil biology (Rein et al. 2008), and this study provides field experimental evidence that this level of severity can be reached at depths up to 30 cm.

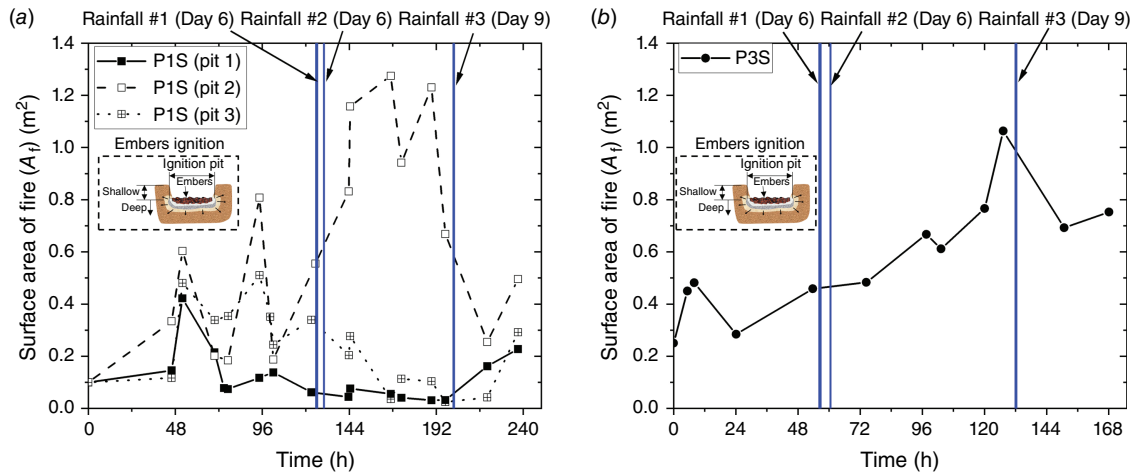
According to infrared images, the surface fire area fluctuated over time (Fig. 10a, before the rainfalls on Day 6). These fluctuations were due to the formation and collapse of overhang. The char layers on top and overhangs (Fig. A7 in the Supplementary Appendix) causing the shape of the fire to change, seemingly indicating a decrease at the surface while the deep layer continues to burn. This can be seen in

Fig. 11 from  $t = 94.5$  to 123.1 h, when the peat fire spread but the surface area seemed to decrease in some parts. However, in P3S, the peat fire surface area steadily increased (Fig. 10b) and with similar severity of smouldering in both shallow and deep layers (Fig. 9d). The different spread behaviour in P3S can be caused by the significantly lower MC than the other plots, as seen in Table 1.

### Comparison of slash-and-burn and ember ignitions

Ember-ignited fire was strongest in deeper layers (Fig. 9c for ember ignition vs Fig. 9a for slash-and-burn). In the shallow layer, the peak temperature due to slash-and-burn was ~700°C and ~470°C for the ember-ignited fire. In the deep layer, the peak temperature due to slash-and-burn was ~580°C and ~550°C for the ember-ignited fire. This might be a result of the ignition method, in which the burning embers were placed in 20–40 cm inside the pits, thus directly igniting the peat below the surface. The most





**Fig. 10.** Surface area of smouldering fires in (a) PIS and (b) P3S measured by infrared imaging. The x-axis time of PIS and P3S are different. Time at 0 h in each plot represents their time of ignition. The last data point represents measurement before controlled suppression on Day 11.

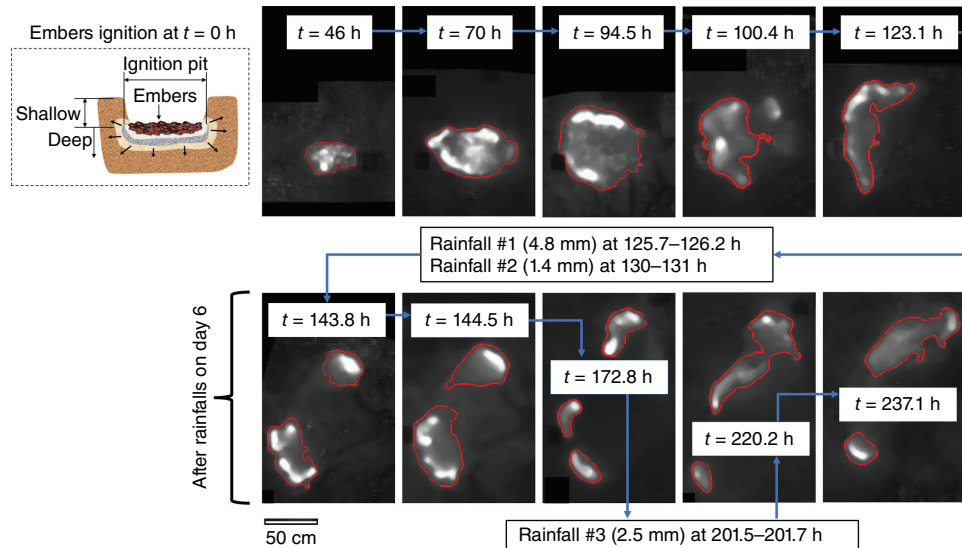


**Fig. 11.** Evolution of a smouldering hotspot at the surface as measured by infrared camera on Pit 3 of PIS from  $t = 46$  to 237.1 h. Time at 0 h is the time of ignition. Rainfalls occurred at  $t = 125.7$ ,  $t = 130$  and  $t = 201.5$  h. The suppression of this fire was at  $t \sim 244$  h.

severe peat fire was in P1S, where the residence time at 200°C or more was up to 40 h (Fig. 9c). The fire in P1S was also the longest in this study, up to 10 days (Fig. 3a).

Continuous measurements of MC in P2N revealed that the flaming from slash-and-burn had a small effect on peat moisture (Fig. 12). Following slash-and-burn, peat MC decreased by ~10% but then returned to previous levels due to water migration over the subsequent 30 h. The small decrease of MC due to slash-and-burn is evidence of the shallow impact of flames on the soil that has been previously discussed in Hartford and Frandsen (1992); Rein *et al.* (2008) and Santoso *et al.* (2019). The drying front ahead of smouldering peat arrives at the sensor’s location with a

very swift decrease in peat MC to ~0% (very dry conditions). The fire spreads downwards from shallow to deep layers; MC at 10 and 20 cm depths decreased first, followed by further decreases of MC at 30 and then at 40 cm depth in the next ~5 and 15 h respectively.

### Smouldering spread during day and night

Smouldering fires in the field have only been observed during the day. Here, we attempt to compare smouldering spread between day and night. Day and night periods are defined as 05:00 to 18:00 hours (13 h) and 18:00 to 05:00 hours (11 h) respectively. The maximum smouldering

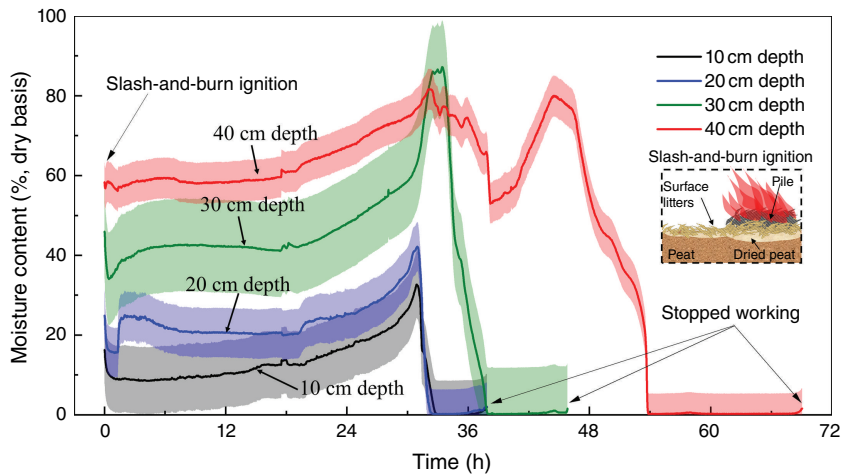


**Fig. 12.** Moisture content measurement as smouldering spread into the location conducted by burying four moisture sensors at 10, 20, 30, and 40 cm depths right below the pile of slash-and-burn in P2N. Cloud represents the uncertainty. The sensors stopped working due to high temperature caused by the approaching fire.

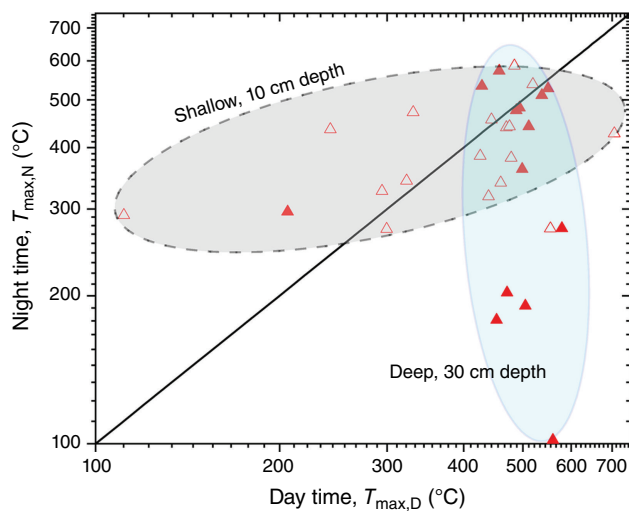


**Fig. 13.** Temperatures in smouldering peat during day and night, represented by maximum values ( $T_{\max}$ ). Subscripts D and N refer to daytime and night-time respectively. Hollow and solid red triangles represent thermocouples placed at 10 and 30 cm depth respectively. Grey shading (dashed line) is an approximate grouping of maximum temperature from thermocouples at 10 cm depth (shallow layer), and cyan shading (solid line) is an approximate grouping of thermocouples at 30 cm depth (deep layer).

temperatures at each thermocouple location in Fig. 8 during each period were then used to analyse fire spread in day and night periods. On average, peat fire during daytime was 20% hotter than night-time, owing to the higher ambient temperature, lower humidity, and longer period of daytime (13 h compared with 11 h of night-time) than those of night-time. See Fig. 13 for maximum smouldering temperature and Fig. A13 in the Supplementary Appendix for average smouldering temperature. At  $\sim 500^{\circ}\text{C}$  during the day and night periods (Fig. 13), the data clusters around the line of  $T_{\max,D} = T_{\max,N}$ , implying that strong fire will persistently spread equally despite changing environmental conditions

between day and night. Fig. 13 also shows that, during daytime, smouldering at deep layer was 13% hotter than shallow layer. During night-time, both smouldering at shallow and deep layers have about the same level of smouldering temperature.

### Smouldering spread in peat with high inorganic content

The mass fractions of C/H/N of the north and south sides of the plots are given in Table 1. Both sides have lower carbon content than typical tropical peat forests, which is  $\sim 55\text{--}60\%$  (Könönen et al. 2015). The inorganic content (IC) of the peat was also high compared with tropical peatland of  $3 \pm 1.96\%$  (Ramadhan et al. 2017). Thus, the peat in GAMBUT site is considerably degraded, meaning that the conditions needed to sustain slow organic decomposition cannot be fully satisfied. Based on three established peat classification systems of International Peat Society (IPS), Canada Soil Survey Committee (CSSC), and International Organization of Standardization (ISO), the soil in this study is classified as peat because the IC is less than 70% (Huang et al. 2009).

Despite the high IC, the peat fire spread persistently over 4–10 days of the field experiment and resulted in a depth of burn of 25 cm on average; and despite three major rain events (Fig. 3a, b), the embers-ignited fire spread up to an area of  $1.3\text{ m}^2$  (Fig. 10a) and with a perimeter up to 9 m. The high IC is partially responsible for the slow horizontal fire spread rate, compared with the literature, which ranges from  $0.5$  to  $19.5\text{ cm h}^{-1}$  (Prat-Guitart et al. 2016b; Christensen et al. 2020; Cowan et al. 2020). Fig. 14 shows the spread rate ( $\bar{S}_1$ ) obtained from thermocouple at 10 cm depth that was from  $0.6$  to  $0.9\text{ cm h}^{-1}$ , with initial MC from 23 to 141% at dry-base.  $\bar{S}_1$  is the average of spread rates based on maximum temperature and  $300^{\circ}\text{C}$  isotherm temperature. Continuous MC measurements revealed a drying front spread rate of  $0.9\text{ cm h}^{-1}$  at depths from 10 to 30 cm,

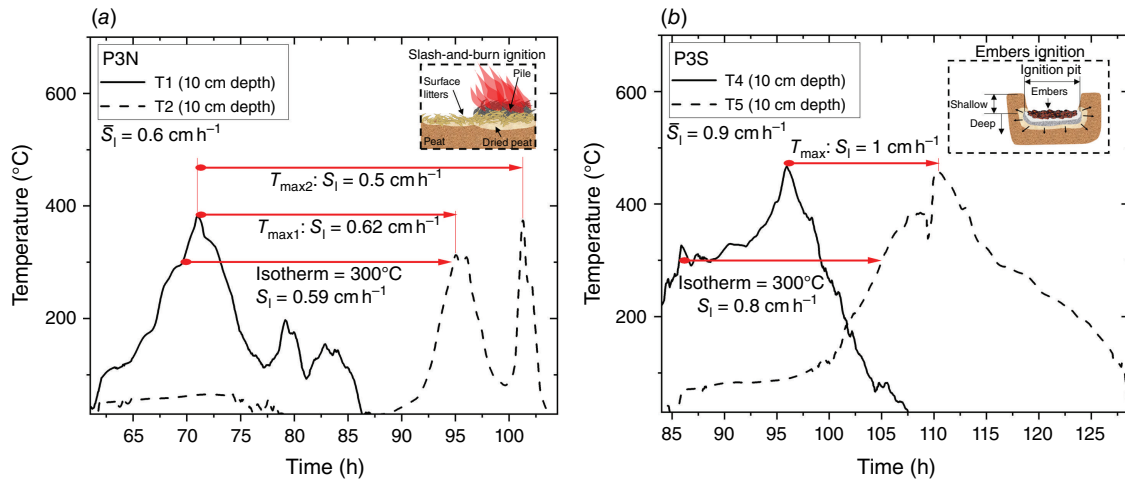


**Fig. 14.** Evolution of smouldering temperatures measured by thermocouple at 10 cm depth in (a) P3N and (b) P3S. For thermocouple locations in P3N, refer to Fig. 8c. For thermocouple locations in P3S, refer to Fig. A6b, Supplementary Appendix. The initial MC of P3N was 141%, with IC of 50% at dry-base. The initial MC of P3S was 23%, with IC of 71% at dry-base. Ignition in P3N and P3S are at 16.2 and 9.45 h respectively.  $S_1$  is smouldering spread rate in the horizontal direction and  $\bar{S}_1$  is the average.

and  $0.6 \text{ cm h}^{-1}$  at depths from 30 to 40 cm (Fig. 12). The small difference between horizontal spread rates despite the wide difference in MC is because the combination of high IC and high bulk density influence the spread rate more than MC.

Results here emphasise the significance of fires in degraded peatlands with high IC. Currently, the literature defines peat based on widely different organic content (OC) thresholds, from 30% (Joosten and Clarke 2002; Minasny *et al.* 2019) to 65% (Page *et al.* 2011), resulting in  $\sim 60\,000 \text{ km}^2$  of difference in peatland area estimations for Indonesia alone. Page *et al.* (2011) estimated  $206\,950 \text{ km}^2$  of peatland area in Indonesia using an OC threshold of 65%, whereas Joosten (2009) estimated  $265\,500 \text{ km}^2$  with a threshold of 30% OC. Our field study proves the fire risks of degraded peatlands with low OC, and both conservation and mitigation plannings should be implemented on this type of peatland.

## Gas emissions

Fig. 15 reports the Emission Factors (EF) of  $\text{CO}_2$ , CO,  $\text{CH}_4$ ,  $\text{NH}_3$ , and HCN from four fire events (ember ignition, slash-and-burn ignition, spread, and suppression). In general, gas emissions differ significantly among different fuel types (Rein 2016; Hu *et al.* 2019). Comparatively, ember ignition has the largest  $\text{CO}_2$  EFs ( $2446.5 \pm 67.8 \text{ g kg}^{-1}$ ), on average 56% higher than those from slash-and-burn, spread, and suppression. This is mainly because  $\text{CO}_2$  EF is proportional to the carbon content of the fuel. The charcoal embers have distinctively higher carbon content (78%) than those from peat (51.3–57.8%) and surface vegetation (55.0%), thus leading to a much higher EF value of  $\text{CO}_2$  (Hu 2019).

Gas emissions during suppression have not been previously reported in the literature and are investigated for the first time in this study. Variability of 3–8 times was found in EF of different species. The EF of CO ranged between  $68.5$  and  $391.4 \text{ g kg}^{-1}$ , with  $\text{CH}_4$  between  $2.9$  and  $9.3 \text{ g kg}^{-1}$ , and  $\text{NH}_3$  between  $1.0$  and  $8.3 \text{ g kg}^{-1}$ . During all stages of the experiment, the average emission factor of CO was  $210 \pm 76.7 \text{ g kg}^{-1}$ , compared with  $\text{CH}_4$ , which was  $4.6 \pm 2.3 \text{ g kg}^{-1}$  and  $\text{NH}_3$ , which was  $3.5 \pm 1.9 \text{ g kg}^{-1}$ . As can be seen in Fig. 15, EFs during spread were relatively similar to those during suppression.

## Rainfall and suppression of peat fires

Three rainfall events occurred during our study, with water column height in the range of  $1.4$ – $4.8 \text{ mm}$  for  $17$ – $60 \text{ min}$  duration (see Fig. 3b). These rainfalls were insufficient to suppress the fire in the deep layer but had a substantial effect on the shallow layer. This effect can be seen in Fig. 11 – after the first two rainfalls, the fire spread weakly in patches. This spread occurred at the surface and was caused by the increased MC at the surface due to rainfalls. However, the fire kept spreading even though the surface MC was increased, indicating that the rainfalls had less effect on the layers below the surface.

After the rainfalls on Day 6 (Fig. 3a, b), the fire area decreased by about 30–40%, except in ignition Pit 2 of P1S (Fig. 10a) and P3S (Fig. 10b), but the fire was not extinguished and continued spreading. The effect of rainfalls on shallow smouldering can be seen in Fig. 11, as the fire perimeter of Pit 3 of P1S decreased by 39% from  $t = 123.1$  to  $143.8 \text{ h}$ . Further spread can be seen afterwards, showing that peat fire at the surface was self-sustained.



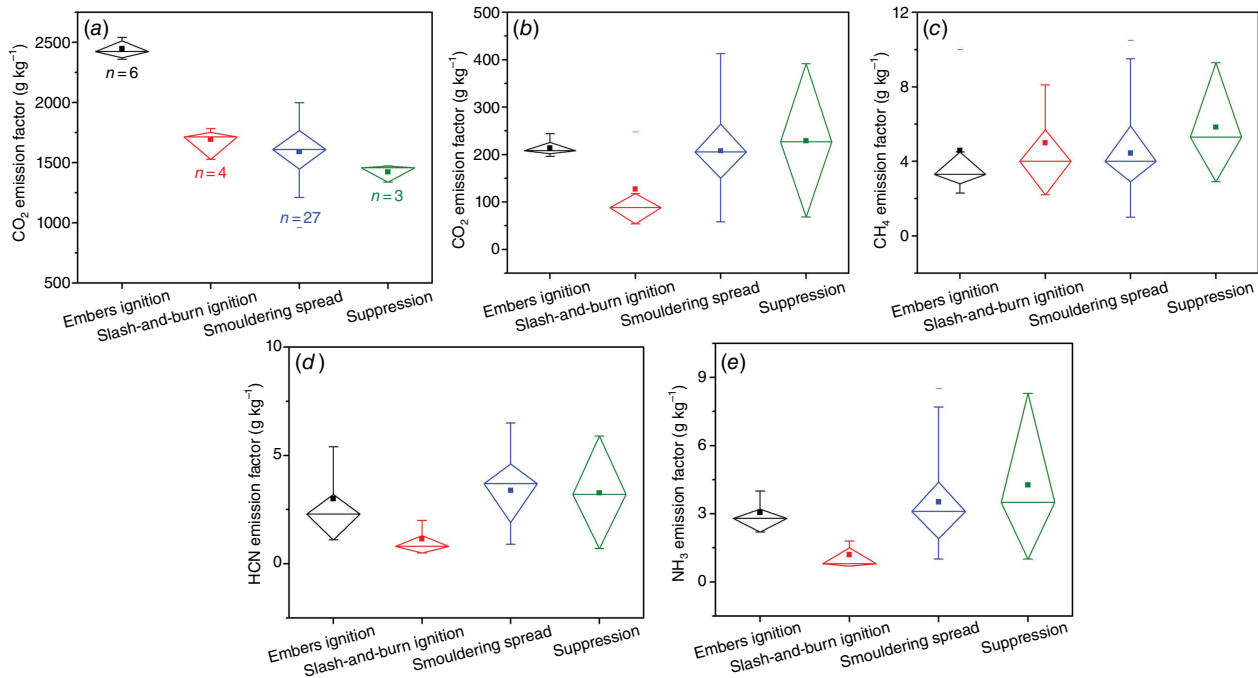


**Fig. 15.** The emission factors of CO<sub>2</sub> (a), CO (b), CH<sub>4</sub> (c), NH<sub>3</sub> (d), and HCN (e) from different stages of the experiment. The mean values are represented by solid squares and are averaged on different measurement locations over 10–110 min (details in Table A1, Supplementary Appendix). The diamond represents emission data of lower quartile (25th percentile), median (50th percentile), and upper quartile (75th percentile). The error bars show the range of values in each experiment stage, and *n* is the number of measurements.

The third rainfall event occurred on Day 9 with a higher rate than the previous rainfalls (Fig. 3b). It affected the fire more than the first two rainfalls as seen in the 62% decrease of fire area of Pit 2 in P1S and 35% in P3S (Fig. 10). Pit 1 of P1S, however, increased weakly after this second rainfall.

Lin *et al.* (2020) reported that the critical rainfall rate to extinguish a peat fire is 4 mm h<sup>-1</sup>, substantially below two of the rainfalls recorded here (see Fig. 3b). However, successful suppression with 4 mm h<sup>-1</sup> requires ~5 h of suppression duration, much longer than the rainfall durations observed, which were from 17 to 60 min. This implies a critical intensity (or flow rate) and duration for a successful suppression. Fig. 16a shows that successful suppression with water spray and injection agree with the critical suppression threshold found in Santoso *et al.* (2021) from laboratory experiments. The rainfall events that were unsuccessful in suppressing peat fires were below the critical threshold of flow rate and duration of suppression, confirming that the rainfall intensity and duration were too low and too short respectively.

Fig. 16b shows that successful suppression occurred above a certain threshold of suppression column height ( $H_s$ , mm), below which the suppression is not successful.  $H_s$  is calculated by using Eqn A1 in the Supplementary Appendix. In this study, the  $H_s$  threshold is 26.5 ± 9.2 mm (water spray suppression in P1N). This value is in the range

of the threshold reported in previous laboratory studies, 13 ± 1.9 mm in Lin *et al.* (2020) and 36 ± 5 mm in Santoso *et al.* (2021). Far below this threshold is the  $H_s$ , due to aforementioned rainfall events that resulted in unsuccessful suppression, i.e. 4.8, 1.4, and 2.5 mm. Suppression by lance injection appears to be an inefficient method due to the significantly higher  $H_s$  when compared with the spray suppression (Fig. 16b), indicating an excess use of water to reach suppression with durations that are not much shorter than water spray (Fig. 16a). This low efficiency of lance injection has been explained previously (Hadden and Rein 2011) as resulting from the high runoff. Considering the low efficiency of this method, but also the merit of attacking a local and in-depth hot spot, lance injection might be more suitable for mopping up residual in-depth and patched hotspots after a large-scale peat fire to avoid rekindling, for example with the aid of infrared imaging.

After the controlled suppression on Day 11, a detailed survey of the plots was conducted on Day 12 to ensure that the peat fire was extinguished in all plots. This survey was conducted by digging for fire in-depth up to the depth of the virgin peat layer. A very small number, two to three, of hot spots were found and were covered by wet layers of ash and char. After digging, the experimental area was sprayed with water again and the experiment was terminated.

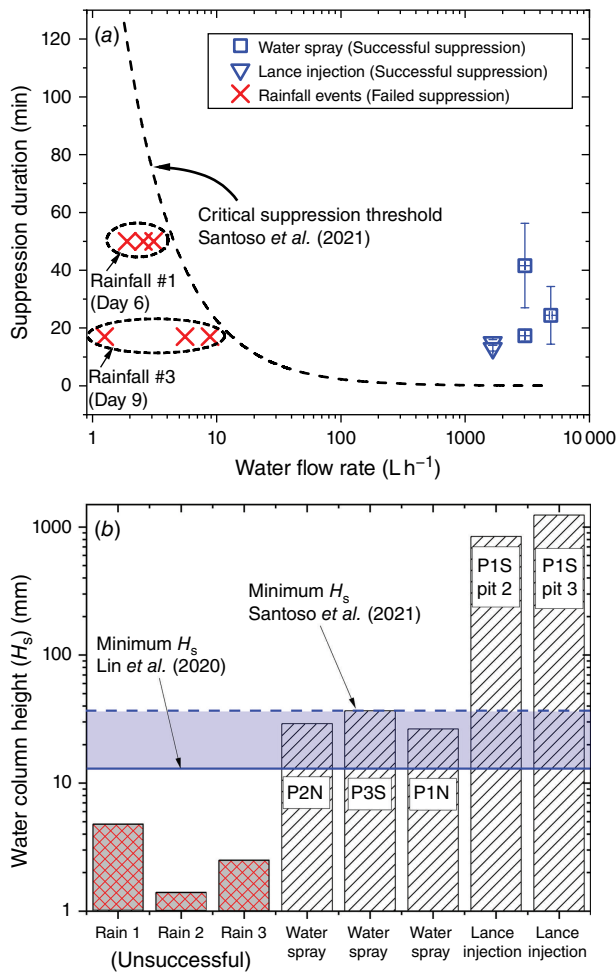


**Fig. 16.** Suppression duration and water column height in GAMBUT. (a) Suppression duration and flow rate of water spray, lance injection, and rainfalls. The dashed line represents the critical suppression threshold from the lab experiment of Santoso et al. (2021). (b) Water column height ( $H_s$ , mm) for the different experiments. Dashed and solid blue lines represent the minimum water column height by Santoso et al. (2021) and Lin et al. (2020) respectively.

## Conclusions

GAMBUT represents the largest and longest to-date field experiment of peat wildfires. The field experiment was conducted on a degraded peatland in Sumatra, Indonesia, in which the smouldering peat burned from 4 to 10 days despite substantial variability in environmental conditions and precipitation. Even though the inorganic and moisture contents of the peat were high, the peat fire spread persistently for up to 10 days of field experiment and resulted in a depth of burn of 25 cm on average. Despite three major rain events, the embers-ignited fire spread up to an area of 1.3 m<sup>2</sup> and with a perimeter up to 9 m. The high inorganic content of the peat, though, substantially lowered the spread rate. This finding calls for caution even in areas with relatively high inorganic content.

Smouldering was found to result in higher temperature in the shallow layers than in the deep layers when ignition was by slash-and-burn. With ignition by ember, smouldering temperature was higher in the deep layers than in the shallow layers. Measurements of temperature in the soil provide field experimental evidence of lethal fire severity to the biological system of the peat up to 30 cm depth.

Smouldering was found to be hotter during daytime than night-time. Daytime maximum soil temperature was up to 20% higher than night-time temperature. This is because of the higher ambient temperature and lower humidity during daytime. The smouldering temperature at deep layer was found to be at the highest during daytime, represented by a deep layer maximum temperature about 13% higher than the shallow layer temperature. During night-time, both deep and shallow layer smouldering had the same level of temperature. This behaviour was not observed before and is important for firefighting responses conducted mostly during daytime.

Gaseous emissions were measured over various stages of the experiment: ignition, smouldering spread, and suppression. Ember ignition had the largest CO<sub>2</sub> emission factor, on average 56% higher than those from slash-and-burn ignition, smouldering peat fire spread, and suppression. Charcoal ember consumed within this fire event had distinctively higher carbon content (78%) than those from peat (51.3–57.8%) and surface vegetation (55.0%).

After rainfall, the surface area of the fire was reduced but kept spreading until the controlled suppressions were conducted at the end of the experiment. This indicates that rainfall events might suppress peat fire in the shallow layers, but not in the deep layers. The water column height that resulted in successful suppression was  $26.5 \pm 9.2$  mm. Agreement of water column height between our field experiment and laboratory-scale experiments in the literature implies that suppression dynamics studied at the lab scale are valuable for guiding mitigation strategies.

Results in this study represent smouldering peat fire dynamics in the field in terms of smouldering temperature, spread rate, thermal residence time, and critical water column height for successful suppression. These results are unique and can be used to develop better mitigation and firefighting responses, which would eventually reduce the global burden of harmful emissions and ecological damage due to peat fires.

## Supplementary material

Supplementary material is available [online](#).

## References

- Amin HMF, Hu Y, Rein G (2020) Spatially resolved horizontal spread in smouldering peat combining infrared and visual diagnostics. *Combustion and Flame* **220**, 328–336. doi:10.1016/j.combustflame.2020.06.039

- Badan Pusat Statistik Kabupaten Rokan Hilir (2015) Rata-Rata Curah Hujan Di Kabupaten Rokan Hilir (mm) 2013–2015. Available at <https://rohilkab.bps.go.id/subject/151/iklim.html#subjekViewTab3> [Verified 27 August 2021]
- Benscoter BW, Thompson DK, Waddington JM, Flannigan MD, Wotton BM, de Groot WJ, Turetsky MR (2011) Interactive effects of vegetation, soil moisture and bulk density on depth of burning of thick organic soils. *International Journal of Wildland Fire* 20(3), 418–429. doi:10.1071/WF08183
- BMKG (2022) Indonesia online climate database. Available at [http://dataonline.bmkg.go.id/data\\_iklim](http://dataonline.bmkg.go.id/data_iklim) [Verified 14 May 2022]
- Chen H, Zhao W, Liu N (2011) Thermal analysis and decomposition kinetics of Chinese forest peat under nitrogen and air atmospheres. *Energy & Fuels* 25(2), 797–803. doi:10.1021/ef101155n
- Christensen E, Hu Y, Restuccia F, Santoso MA, Huang X, Rein G (2019) Experimental methods and scales in smouldering wildfires. In 'Fire Effects on Soil Properties'. (Eds P Pereira, J Mataix-Solera, X Ubeda, G Rein, A Cerdà) pp. 267–280. (CSIRO Publishing: Melbourne, Vic., Australia)
- Christensen EG, Fernandez-Anez N, Rein G (2020) Influence of soil conditions on the multidimensional spread of smouldering combustion in shallow layers. *Combustion and Flame* 214, 361–370. doi:10.1016/J.COMBUSTFLAME.2019.11.001
- Cowan DA, Page WG, Butler BW, Blunck DL (2020) Effects of fuel characteristics on horizontal spread rate and ground surface temperatures of smouldering duff. *International Journal of Wildland Fire* 29(9), 820–831. doi:10.1071/WF19207
- Frandsen WH (1987) The influence of moisture and mineral soil on the combustion limits of smouldering forest duff. *Canadian Journal of Forest Research* 17(12), 1540–1544. doi:10.1139/x87-236
- Frandsen WH (1997) Ignition probability of organic soils. *Canadian Journal of Forest Research* 27, 1471–1477. doi:10.1139/x97-106
- Gandois L, Hoyt AM, Hatté C, Jeanneau L, Teisserenc R, Liotaud M, Tananaev N (2019) Contribution of peatland permafrost to dissolved organic matter along a thaw gradient in North Siberia. *Environmental Science & Technology* 53(24), 14165–14174. doi:10.1021/acs.est.9b03735
- Gaveau DLA, Salim MA, Hergoualc'h K, Locatelli B, Sloan S, Wooster M, Marlier ME, Molidena E, Yaen H, DeFries R, Verchot L, Murdiyarso D, Nasi R, Holmgren P, Sheil D (2014) Major atmospheric emissions from peat fires in southeast Asia during non-drought years: evidence from the 2013 Sumatran fires. *Scientific Reports* 4(1), 6112. doi:10.1038/srep06112
- Hadden R, Rein G (2011) Burning and water suppression of smoldering coal fires in small-scale laboratory experiments. In 'Coal and Peat Fires: A Global Perspective'. (Eds GB Stracher, A Prakash, G Rein) pp. 317–326. (Elsevier: Amsterdam, The Netherlands) doi:10.1016/B978-0-444-52858-2.00018-9
- Hartford RA, Frandsen WH (1992) When it's hot, it's hot... or maybe it's not! (surface flaming may not portend extensive soil heating). *International Journal of Wildland Fire* 2(3), 139–144. doi:10.1071/WF9920139
- Hoyt AM, Chaussard E, Seppalainen SS, Harvey CF (2020) Widespread subsidence and carbon emissions across southeast Asian peatlands. *Nature Geoscience* 13(6), 435–440. doi:10.1038/s41561-020-0575-4
- Hu Y (2019) Experimental Investigation of Peat Fire Emissions and Haze Phenomena. PhD thesis, Imperial College, London, UK.
- Hu Y, Fernandez-Anez N, Smith TEL, Rein G (2018) Review of emissions from smouldering peat fires and their contribution to regional haze episodes. *International Journal of Wildland Fire* 27(5), 293–312. doi:10.1071/WF17084
- Hu Y, Christensen EG, Amin HMF, Smith TEL, Rein G (2019) Experimental study of moisture content effects on the transient gas and particle emissions from peat fires. *Combustion and Flame* 209, 408–417. doi:10.1016/j.combustflame.2019.07.046
- Huang X, Rein G (2014) Smouldering combustion of peat in wildfires: inverse modelling of the drying and the thermal and oxidative decomposition kinetics. *Combustion and Flame* 161, 1633–1644. doi:10.1016/j.combustflame.2013.12.013
- Huang X, Rein G (2019) Upward-and-downward spread of smoldering peat fire. *Proceedings of the Combustion Institute* 37(3), 4025–4033. doi:10.1016/j.proci.2018.05.125
- Huang PT, Patel M, Santagata MC, Bobet A (2009) 'Classification of Organic Soils.' (Purdue University: West Lafayette, IN, USA)
- Huang X, Restuccia F, Gramola M, Rein G (2016) Experimental study of the formation and collapse of an overhang in the lateral spread of smouldering peat fires. *Combustion and Flame* 168, 393–402. doi:10.1016/J.COMBUSTFLAME.2016.01.017
- Huijnen V, Wooster MJ, Kaiser JW, Gaveau DLA, Flemming J, Parrington M, Inness A, Murdiyarso D, Main B, van Weele M (2016) Fire carbon emissions over maritime Southeast Asia in 2015 largest since 1997. *Scientific Reports* 6(1), 26886. doi:10.1038/srep26886
- Iriana W, Tonokura K, Inoue G, Kawasaki M, Kozan O, Fujimoto K, Ohashi M, Morino I, Someya Y, Imasu R, Rahman MA, Gunawan D (2018) Ground-based measurements of column-averaged carbon dioxide molar mixing ratios in a peatland fire-prone area of central Kalimantan, Indonesia. *Scientific Reports* 8(1), 8437. doi:10.1038/s41598-018-26477-3
- IUCN (2017) Peatlands and climate change: issues brief. Available at <https://www.iucn.org/resources/issues-briefs/peatlands-and-climate-change> [Verified 27 August 2021]
- Joosten H (2009) 'The Global Peatland CO2 Picture: Peatland Status and Drainage Related Emissions in All Countries of the World.' (Wetlands International) Available at [https://unfccc.int/files/kyoto\\_protocol/application/pdf/draftpeatlandco2report.pdf](https://unfccc.int/files/kyoto_protocol/application/pdf/draftpeatlandco2report.pdf) [Verified 27 August 2021]
- Joosten H, Clarck D (2002) 'Wise Use of Mires and Peatlands'. p. 304. (International Mire Conservation Group and International Peat Society)
- Kelly R, Chipman ML, Higuera PE, Stefanova I, Brubaker LB, Hu FS (2013) Recent burning of boreal forests exceeds fire regime limits of the past 10,000 years. *Proceedings of the National Academy of Sciences* 110(32), 13055–13060. doi:10.1073/pnas.1305069110
- Könönen M, Jauhiainen J, Laiho R, Kusin K, Vasander H (2015) Physical and chemical properties of tropical peat under stabilised land uses. *Mires and Peat* 16, 1–13.
- Lin S, Cheung YK, Xiao Y, Huang X (2020) Can rain suppress smoldering peat fire? *Sci Total Environ* 727, 138468–. doi:10.1016/j.scitotenv.2020.138468
- Mickler RA, Welch DP, Bailey AD (2017) Carbon emissions during wildland fire on a North American temperate peatland. *Fire Ecology* 13(1), 34–57. doi:10.4996/fireecology.1301034
- Minasny B, Berglund Ö, Connolly J, Hedley C, de Vries F, Gimona A, Kempen B, Kidd D, Lilja H, Malone B, McBratney A, Roudier P, O'Rourke S, Rudiyanto, Padarian J, Poggio L, ten Caten A, Thompson D, Tuve C, Widyatmanti W (2019) Digital mapping of peatlands – a critical review. *Earth-Science Reviews* 196, 102870. doi:10.1016/j.earscirev.2019.05.014
- Muñoz-Rojas M, Bárcenas-Moreno G (2019) Microbiology. In 'Fire Effects on Soil Properties'. (Eds P Pereira, J Mataix-Solera, X Ubeda, G Rein, A Cerdà) pp. 157–74. (CSIRO Publishing: Melbourne, Vic., Australia)
- Murdiyarso D, Saragi-Sasmito MF, Rustini A (2019) Greenhouse gas emissions in restored secondary tropical peat swamp forests. *Mitigation and Adaptation Strategies for Global Change* 24, 507–520. doi:10.1007/s11027-017-9776-6
- Ohlemiller TJ (1985) Modeling of smoldering combustion propagation. *Progress in Energy and Combustion Science* 11(4), 277–310. doi:10.1016/0360-1285(85)90004-8
- Page SE, Siegert F, Rieley JO, Boehm H-DV, Jaya A, Limin S (2002) The amount of carbon released from peat and forest fires in Indonesia during 1997. *Nature* 420(6911), 61–65. doi:10.1038/nature01131
- Page SE, Rieley JO, Banks CJ (2011) Global and regional importance of the tropical peatland carbon pool. *Global Change Biology* 17(2), 798–818. doi:10.1111/j.1365-2486.2010.02279.x
- Pastor E, Oliveras I, Urquiaga-Flores E, Quintano-Loayza JA, Manta MI, Planas E (2017) A new method for performing smouldering combustion field experiments in peatlands and rich-organic soils. *International Journal of Wildland Fire* 26(12), 1040–1052. doi:10.1071/WF17033
- Paton-Walsh C, Smith TEL, Young EL, Griffith DWT, Guérette ÉA (2014) New emission factors for Australian vegetation fires measured using open-path Fourier Transform Infrared Spectroscopy – Part 1: methods



- and Australian temperate forest fires. *Atmospheric Chemistry and Physics* 14(20), 11313–11333. doi:10.5194/acp-14-11313-2014
- Prat-Guitart N, Rein G, Hadden RM, Belcher CM, Yearsley JM (2016a) Effects of spatial heterogeneity in moisture content on the horizontal spread of peat fires. *Science of the Total Environment* 572, 1422–1430. doi:10.1016/j.scitotenv.2016.02.145
- Prat-Guitart N, Rein G, Hadden RM, Belcher CM, Yearsley JM (2016b) Propagation probability and spread rates of self-sustained smouldering fires under controlled moisture content and bulk density conditions. *International Journal of Wildland Fire* 25(4), 456–465. doi:10.1071/WF15103
- Purnomo DMJ, Bonner M, Moafi S, Rein G (2021) Using cellular automata to simulate field-scale flaming and smouldering wildfires in tropical peatlands. *Proceedings of the Combustion Institute* 38(3), 5119–5127. doi:10.1016/j.proci.2020.08.052
- Ramadhan ML, Palamba P, Imran FA, Kosasih EA, Nugroho YS (2017) Experimental study of the effect of water spray on the spread of smoldering in Indonesian peat fires. *Fire Safety Journal* 91, 671–679. doi:10.1016/J.FIRESAF.2017.04.012
- Rein G (2013) Smouldering fires and natural fuels. In 'Fire Phenomena and the Earth System'. (Ed. CM Belcher) pp. 15–33. (John Wiley & Sons: Chichester, UK.)
- Rein G (2016) Smoldering combustion. In 'SFPE Handbook of Fire Protection Engineering'. (Eds MJ Hurley, D Gottuk, JR Hall, K Harada, E Kuligowski, M Puchovsky, J Torero, JM Watts, C Wieczorek) pp. 581–603. (Springer: New York, NY, USA)
- Rein G, Huang X (2021) Smouldering wildfires in peatlands, forests and the arctic: challenges and perspectives. *Current Opinion in Environmental Science & Health* 24, 100296. doi:10.1016/j.coesh.2021.100296
- Rein G, Cleaver N, Ashton C, Pironi P, Torero JL (2008) The severity of smouldering peat fires and damage to the forest soil. *CATENA* 74(3), 304–309. doi:10.1016/J.CATENA.2008.05.008
- Restuccia F, Huang X, Rein G (2017) Self-ignition of natural fuels: can wildfires of carbon-rich soil start by self-heating? *Fire Safety Journal* 91, 828–834. doi:10.1016/J.FIRESAF.2017.03.052
- Rieley J, Page S (2016) Tropical peatland of the world. In 'Tropical Peatland Ecosystems'. (Eds M Osaki, N Tsuji) pp. 3–32. (Springer: Tokyo, Japan)
- Santoso MA, Huang X, Prat-Guitart N, Christensen E, Hu Y, Rein G (2019) Smouldering fires and soils. In 'Fire Effects on Soil Properties'. (Eds P Pereira, J Mataix-Solera, X Ubeda, G Rein, A Cerdà) pp. 203–216. (CSIRO Publishing: Melbourne, Vic., Australia)
- Santoso MA, Cui W, Amin HMF, Christensen EG, Nugroho YS, Rein G (2021) Laboratory study on the suppression of smouldering peat wildfires: effects of flow rate and wetting agent. *International Journal of Wildland Fire* 30(5), 378–390. doi:10.1071/WF20117
- See SW, Balasubramanian R, Rianawati E, Karthikeyan S, Streets DG (2007) Characterization and source apportionment of particulate matter  $\leq 2.5$  Mm in Sumatra, Indonesia, during a recent peat fire episode. *Environmental Science & Technology* 41(10), 3488–3494. doi:10.1021/es061943k
- Simpson JE, Wooster MJ, Smith TEL, Trivedi M, Vernimmen RRE, Dedi R, Shakti M, Dinata Y (2016) Tropical peatland burn depth and combustion heterogeneity assessed using UAV photogrammetry and airborne LiDAR. *Remote Sensing* 8(12), 1000. doi:10.3390/rs8121000
- Smith TEL, Paton-Walsh C, Meyer CP, Cook GD, Maier SW, Russell-Smith J, Wooster MJ, Yates CP (2014) New emission factors for Australian vegetation fires measured using open-path Fourier Transform Infrared Spectroscopy – Part 2: Australian tropical savanna fires. *Atmospheric Chemistry and Physics* 14(20), 11335–11352. doi:10.5194/acp-14-11335-2014
- Smith TEL, Evers S, Yule CM, Gan JY (2018) In situ tropical peatland fire emission factors and their variability, as determined by field measurements in Peninsula Malaysia. *Global Biogeochemical Cycles* 32(1), 18–31. doi:10.1002/2017GB005709
- Tacconi L (2016) Preventing fires and haze in Southeast Asia. *Nature Climate Change* 6(7), 640–643. doi:10.1038/nclimate3008
- Torero JL, Fernandez-Pello AC (1996) Forward smolder of polyurethane foam in a forced air flow. *Combustion and Flame* 106(1), 89–109. doi:10.1016/0010-2180(95)00245-6
- Turetsky MR, Benscoter B, Page S, Rein G, van der Werf GR, Watts A (2015) Global vulnerability of peatlands to fire and carbon loss. *Nature Geoscience* 8(1), 11–14. doi:10.1038/ngeo2325
- Usup A, Hashimoto Y, Takahashi H, Hayasaka H (2004) Combustion and thermal characteristics of peat fire in tropical peatland in central Kalimantan, Indonesia. *Tropics* 14, 1–19. doi:10.3759/tropics.14.1
- Walker XJ, Rogers BM, Veraverbeke S, Johnstone JF, Baltzer JL, Barrett K, Bourgeau-Chavez L, Day NJ, de Groot WJ, Dieleman CM, Goetz S, Hoy E, Jenkins LK, Kane ES, Parisien MA, Potter S, Schuur EAG, Turetsky M, Whitman E, Mack MC (2020) Fuel availability not fire weather controls boreal wildfire severity and carbon emissions. *Nature Climate Change* 10, 1130–1136. doi:10.1038/s41558-020-00920-8
- Yu ZC (2012) Northern peatland carbonstocks and dynamics: a review. *Biogeosciences* 9(10), 4071–4085. doi:10.5194/bg-9-4071-2012

**Data availability.** The datasets of the current study are available from the corresponding author on reasonable request.

**Conflicts of interest.** The authors declare no conflicts of interest.

**Declaration of funding.** This study was funded by: the Engineering and Physical Sciences Research Council Global Challenges Research Fund GAMBUT (United Kingdom); European Research Council Consolidator grant Haze (682587); Ministry of Research, Technology, and Higher Education of the Republic of Indonesia and Universitas Indonesia Penelitian Terapan Unggulan Perguruan Tinggi 2018–2020 (514/UN2.R3.I/HKP05.00/2018); Hibah Publikasi Q1 Q2 of Universitas Indonesia (Grant ID. NKB-0331/UN2.R3.I/HKP.05.00/2019); Lembaga Pengelola Dana Pendidikan Indonesia Doctorate Scholarship (Republic of Indonesia); Ministry of Internal Affairs of the Republic of Indonesia; The Natural Environment Research Council Field Spectroscopy Facility (United Kingdom); National Natural Science Foundation of China (NSFC) No. 52106184; and Sichuan Fire Research Institution Basic Research Funds No. 20218801z.

**Acknowledgements.** We thank the many collaborators and colleagues who provided vital support to GAMBUT along the way. We are particularly thankful to the team in the field from Universitas Indonesia: Mad Yasin and Dr. Hafizha Mulyasih; from Balai Diklat Satpol PP dan Damkar Rokan Hilir (Kementerian Dalam Negeri Republik Indonesia): Setiawan S. Ag., MSi., Chairullah, Chandra Dorman Lolle, Dedi Hariyanto, Iskandar, Parison, and Rizal; from Universitas Riau: Prof. Ari Sandhyavitri, Dr. Awaluddin Martin, Harun Orion Purba, Yogi Wibowo Agusta, Rizki Ramadhan Husaini, Guspi, Muhamad Yusa, Doni, Jamal; and from local workers in Rokan Hilir: Adnan and team, and Herman. We thank the team remotely assisted from Imperial College London: Dr. Francesco Restuccia, Dr. Guoxiang Zhao, Dr. Han Yuan, Dr. Xuanze He, and Dr. Nieves Fernandez Anes; and from Universitas Indonesia in Depok: Jefri Alfonso Sigalingging, Nadhira Gilang Ratnasari, Aditya Hartawan, and Hanifa Khansa Zhafira. We are deeply grateful for the fruitful discussions and advice from experts in Indonesia: Dr. Rizari (Kementerian Dalam Negeri Republik Indonesia); Evan Nur Setya Hadi, S.STP, M.AP. (Kementerian Dalam Negeri Republik Indonesia); Prof. Bambang Hero (Institut Pertanian Bogor); and Dr. Haris Gunawan (Peatland Restoration Agency).

#### **Author affiliations**

<sup>A</sup>Department of Mechanical Engineering, and Leverhulme Centre for Wildfires, Environment and Society, Imperial College London, London, SW7 2AZ, UK.

<sup>B</sup>School of Computing, Engineering & Digital Technologies, Teesside University, Middlesbrough, UK.

<sup>C</sup>Department of Mechanical Engineering, Universitas Cenderawasih, Jayapura, Indonesia.

<sup>D</sup>Sichuan Fire Research Institute of the Ministry of Emergency Management, Chengdu, China.

<sup>E</sup>Department of Mechanical Engineering, Universitas Indonesia, 16424, West Java, Indonesia.

<sup>F</sup>Department of Geography & Environment, London School of Economics & Political Science, London, UK.